Diagnostics of Gas Turbine Systems Using Gas Path Analysis and Rotordynamic Response Approach

Gbanaibolou Jombo[1], Suresh Sampath[1], Iain Gray[1]

[1]School of Aerospace, Transport & Manufacturing, Cranfield University, UK

ABSTRACT

The modern gas turbine is plagued with issues centred on improving engine availability and limiting component degradation. The integrated use of different condition monitoring techniques presents a solution to addressing these challenges. This paper lays a foundation for the integration of gas path analysis and the rotordynamic response of the compressor to monitor the effect of fouling in the compressor. In investigating the resultant interaction between the aerodynamic and rotordynamic domain in a compressor caused by fouling, an approach involving the interaction of four different models is explored. The first model, a gas turbine engine performance model is used to simulate a fouled compressor and quantify the extent of performance deterioration with gas path analysis. The extent of performance deterioration from the engine performance model represented by scaling of the compressor maps becomes an input in the second model, a Moore-Greitzer compression system model, which evaluates the disturbed flow field parameters in the fouled compressor. The third model, a momentum-based aerodynamic force model, predicts the fouling induced aerodynamic force based on the disturbed flow field parameters. The aerodynamic force acting as a forcing function in the fourth model, a compressor rotordynamic model, produces the vibration response. From the investigation carried out in this work, it is observed, as the rate of fouling increases in the compressor, typified by a decrease in compressor massflow, pressure ratio and isentropic efficiency, there is a corresponding increase in the vibration amplitude at the first fundamental frequency of the compressor.

Keywords: Moore-Greitzer Model; Compressor Fouling; GPA

NOMENCLATURE

CN	Corrected Non-dimensional speed line
ETA	Isentropic Efficiency
FP	Fouling Parameter
GPA	Gas Path Analysis
LGPA	Linear Gas Path Analysis
NGPA	Non-linear Gas Path Analysis
NDMF	Non-Dimensional Mass Flow
PR	Pressure Ratio

Symbols

a, b	Amplitudes of the disturbed flow coefficient
A, A_c	Resultant amplitude of the disturbed flow coefficient, compressor flow through area
B	Greitzer B-parameter
$(F_{tu})_i, (F_{pr})_i, (F_{un})_i$	Non-dimensional turning, pressure & unsteady momentum forces
$F_{ae}, \bar{F}_{ae}$	Non-dimensional & dimensional total aerodynamic forces
H, W	Parameters from curve fitting the compressor pressure-rise characteristic
N	Number of blade row stages
$m, \dot{m}, M_y, M_x$	Mass of rotor, corrected massflow, bending moment on the y and x-axis
l, l_c	Blade chord, Non-dimensional effective compressor

	& duct flow path length
P, P_1	Plenum pressure-rise coefficient, compressor inlet pressure
Q	Average rescaled flow coefficient
Q_T	Throttle characteristic
R	Compressor wheel mean radius
S	Aspect ratio of the pressure-rise characteristic
$\{S\}_i$	Complex state vector at i-th location along rotor
$[U], U$	Overall complex system matrix, compressor rotational speed
x, y	Vibration displacement in x & y axis
Ψ	Compressor pressure-rise coefficient
Φ	Compressor annulus averaged axial flow coefficient
ξ	Non-dimensional time
γ	Throttle coefficient, stagger angle
$\bar{\psi}_c^c, \bar{\psi}_c^{cc}, \bar{\psi}_c^{cs}$	Integrated compressor characteristics
μ, λ	Compressor inertia parameters $\{\mu = (2Nl)/(R\cos\gamma), \lambda = (Nl)/(R\cos\gamma)\}$
η^*	Phase angle of the amplitudes of disturbed flow coefficients
ψ_{cf}	Fouling sensitivity coefficient
ψ_{co}	Shut-off value of the compressor pressure-rise characteristic
$\Delta MF, \Delta PR$	Relative change in massflow and pressure ratio respectively
$\tau_{c1}, \tau_{c2}, \tau_{c3}$	Compressor torque characteristic coefficients
$\lambda_{tu}, \lambda_{pr}, \lambda_{un}$	Scale factor for turning, pressure and unsteady momentum forces
χ	Aerodynamic-Rotordynamic coupling
Ω	Rotor rotational speed
φ, θ	Shaft bending slopes
ρ	Density of air

1.0 INTRODUCTION

Gas turbine technology has drastically evolved during the past decades, with higher turbine entry temperature, 3D twisted compressor blade, dry low NOx emissions combustor, advanced cooling systems for components, the use of advanced and exotic materials, etc. [1]

However, the consequence of these advances in the modern gas turbine is experienced in reduced engine availability and decrease in component life [2,3]. Thus, it becomes necessary for the gas turbine operator to be able to detect and correct damaging conditions quickly and efficiently. Gas turbine condition monitoring, which involves the use of a variety of techniques such as performance monitoring, vibration analysis, oil analysis, etc. to monitor any significant change in the gas turbine engine operating parameters which is indicative of a developing fault, provides one of such means to address the issue of engine availability improvement and limiting component degradation [2–4].

Although in literature, several techniques for the condition monitoring of gas turbines have been discussed [2,4], the focus has mostly been on the independent application of techniques. This paper focuses on the integration of condition monitoring techniques for gas turbine diagnostics.

The benefits that accrue from integrating different condition monitoring techniques for gas turbine system diagnostics includes improving fault diagnosis confidence and localizing the root cause of complex faults. Meher-Homji et al [3] reports three cases, the overhaul of an offshore gas turbine compressor train, industrial gas turbine exhibiting bearing sub-harmonic resonance and random vibration trips on a centrifugal turbocharger, where performance and vibration data where used to effectively diagnose and localize the faults . Meher-Homji and Focke [5] investigated the use of vibration and performance monitoring for the reduction of gas turbine blading problems . Biliotti et al. [6] looked at the use of vibration and performance monitoring to study the rotating stall behaviour of centrifugal compressors in order to improve their minimum stable flow limit.

Gas path analysis and vibration response analysis are two well established condition monitoring techniques for gas turbine system diagnostics [3]; this paper would address their integration for the investigation of compressor fouling degradation, a fault which is estimated to account for 70% - 85% of the gas turbine performance degradation [7].

Compressor fouling is caused by the deposition of airborne contaminates on the surface of the compressor blades, stators and annulus walls [8]. The effect of fouling on the performance of a gas turbine is manifested in reduced compressor massflow, pressure ratio and isentropic efficiency.

The rate of compressor fouling is affected by the type of environment, location and prevailing atmospheric condition [9]. The effect of fouling and the resulting performance losses can be controlled by a combination of an effective inlet filtration system with a complementary mix of offline and online compressor washing.

2.0 METHODOLOGY

Figure 1 shows an overview of the methodology used in this work to investigate the interaction between the aerodynamic and rotordynamic domain in a fouled compressor. The existence of an interaction between the aerodynamic and rotordynamic domain in a compressor has been reported by Alford [10], Weigl [11] and Tryfonidis et al. [12].

The methodology adopted involves an interaction between four different models: Engine performance model, Moore-Greitzer [13] compression system model, Al-Nahwi [14] aerodynamic force model and 2D transfer matrix rotordynamic model. This approach is based on the premise that, the effect of fouling in the compressor is evident by the scaling of the compressor maps, which also indicates a change in the compressor aerodynamic force leading to changes in the compressor vibration response.

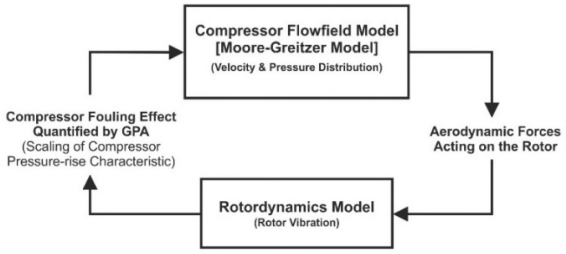

Figure 1 Methodology for investigating the aerodynamic-rotordynamic interaction in a fouled gas turbine compressor

2.1 Engine Performance Model

The engine performance model is based on the thermodynamics of a gas turbine engine. It serves two purposes, firstly, it is used to determine the compressor maps and also used in combination with GPA to quantify the extent of engine fouling degradation.

The GPA results i.e. relative reduction in massflow, pressure ratio and isentropic efficiency are required inputs into the compression system model.

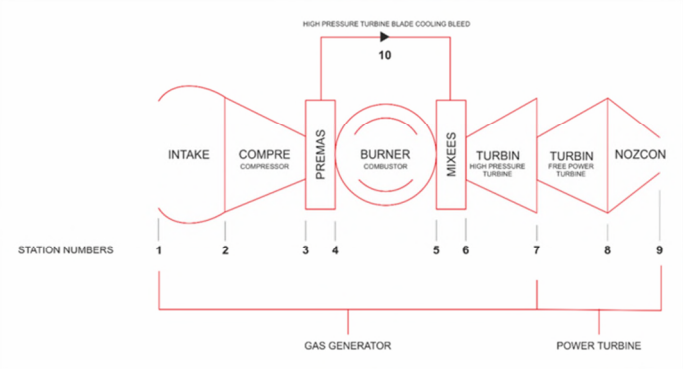

Figure 2 Schematic of a TurboMatch engine model inspired by LM2500+

As shown in Figure 2, a virtual gas turbine performance engine model inspired by the LM2500+ engine with performance parameters given in Table 1 have been modelled in TurboMatch (Cranfield University gas turbine performance software) and the various compressor fouling conditions presented in Table 2 implanted in Pythia (Cranfield University gas turbine diagnostic software) for gas path analysis.

In practice, GPA would be performed on operating data to quantify the extent of the fouling degradation without prior knowledge of such information. In this work, due to the lack of field data, GPA has been performed to confirm the presence of an implanted fouling degradation in a simulated fouled compressor.

Table 1
Design point performance parameters of simulated engine

Parameter	Value	Parameter	Value
Intake			
Ambient temperature	288.15K	Ambient pressure	1.01325 bar
Total pressure recovery	99.5%	Intake mass flow	84.1 kg/s
Compressor			
Compressor efficiency	84%	Compressor pressure ratio	23.1
Compressor exit temperature	769.57K	Number of stages	17
Burner			
Combustion efficiency	99.8%	Burner pressure loss	5%
Fuel flow	1.71kg/s	Thermal efficiency	37.9%
Turbine (Compressor)			
Turbine inlet temperature	1500K	Turbine efficiency	87%
Turbine (Free Power)			
Turbine inlet temperature	805.82K	Turbine efficiency	87%
Net power output	30.39MW	Exhaust gas temperature	805.82K

Table 2
Fouled compressor operating conditions

Cases	% ΔNDMF Reduction	% ΔPR Reduction	% ΔETA Reduction
Case 0 (Clean Engine)	0%	0%	0%
Case 1	1%	1%	1%
Case 2	2%	2%	1%
Case 3	3%	3%	1%
Case 4	4%	4%	1%
Case 5	5%	5%	1%

To confirm the extent of the implanted compressor fouling degradation in the simulated engine, both linear and non-linear gas path analysis has been performed in Pythia. The results for Case 1 and Case 5 is presented in Figure 3 and Figure 4 respectively.

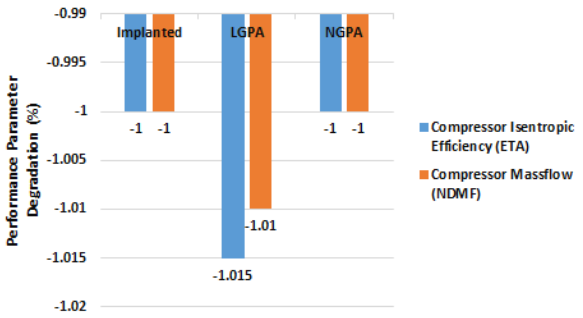

Figure 3 GPA for Case 1

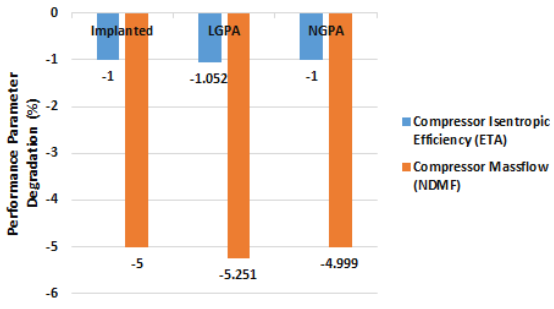

Figure 4 GPA for Case 5

2.2 Moore-Greitzer Compression System Model

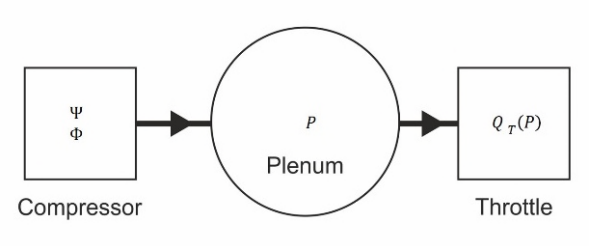

Figure 5 Schematic of the Moore-Greitzer compression system

The Moore-Greitzer compression system model as shown in Figure 5 is a lumped parameter model consisting of a compressor operating in a duct, discharging to a plenum and controlled by a throttle [13].

The Moore-Greitzer compression system model is useful in the prediction of the flowfield parameters in a compressor due to the presence of a disturbance e.g. Surge, stall, etc. It has been used successfully by several investigators in the modelling and control of stall, surge and rotordynamic instabilities in compressors [15–18].

For this work, it is used to determine the amplitudes of the disturbed flow coefficient in the compressor due to fouling.

The governing equations for the Moore-Greitzer compression system are [13,14]:

$$\frac{d\Psi}{d\xi} = \frac{1}{2SB^2 l_c}[\mathrm{Q} - Q_T(P)] \qquad \ldots (\ 1\ )$$

$$\frac{d\Phi}{d\xi} = \frac{S}{2l_c}[\bar{\psi}_c^c(Q,a,b) - P] \qquad \ldots (\ 2\ )$$

$$\frac{d\mathrm{a}}{d\xi} = \frac{1}{(2+\mu)}\left[\frac{S}{2}\bar{\psi}_c^{cc}(Q,a,b) - \lambda b\right] \qquad \ldots (\ 3\ )$$

$$\frac{d\mathrm{b}}{d\xi} = \frac{1}{(2+\mu)}\left[\frac{S}{2}\bar{\psi}_c^{cs}(Q,a,b) + \lambda a\right] \qquad \ldots (\ 4\ )$$

where $Q_T(P) = \gamma\sqrt{P}$.

The steady state solution for Equations (1) – (4) for the amplitudes of the disturbed flow coefficient (a & b) in a fouled compressor is given as [19]:

$$\mathrm{A}^6 + 8Q(Q-1)A^4 + \left[16Q^2(Q-1)^2 + \left(\frac{2\lambda}{3S}\right)^2\right]A^2 - \left[\frac{FP}{6}\right]^2 = \qquad \ldots (\ 5\ )$$

where

$$A = \sqrt{a^2+b^2}\,; a \approx A\cos\eta^*\,; b \approx A\sin\eta^*\,; \qquad \ldots (\ 5\ )$$

$$\eta^* = \sin^{-1}\left(\frac{4\mathrm{A}}{(\mathrm{FP})}\frac{\lambda}{S}\right) \qquad \ldots (\ 6\ )$$

$$FP = \psi_{cf} \times \Delta MF = \left(2 + \frac{\psi_{co}}{H}\right)\Delta PR \qquad \ldots (\ 7\ )$$

2.3 Aerodynamic Force Model

According to Al-Nahwi et al. [14], there are three contributions to the total aerodynamic force acting on the compressor rotor.

The first is the turning force F_{tu}, which occurs due to the presence of a non-uniform circumferential distribution of the axial flow coefficient around the rotor. The second is the pressure force F_{pr}, which is due to the hydrostatic pressure distribution around the rotor and the third is the unsteady momentum force F_{un}, which is due to the unsteady momentum storage within the rotor.

The general expressions for the aerodynamic force components are [14]:

Turning force

$$(F_{tu})_i = \frac{1}{4}\lambda_{tu}\{[bF'_{tu}(Q,a,b)]\boldsymbol{i} + [-aF'_{tu}(Q,a,b)]\boldsymbol{j}\} \quad \ldots (\ 8\ )$$

where

$$F'_{tu}(Q,a,b) = \tau_{c1} + 2\tau_{c2}Q + 3\tau_{c3}\left[Q^2 + \frac{1}{4}(a^2+b^2)\right] \quad \ldots (\ 9\ )$$

Pressure force

$$\left(F_{pr}\right)_i = \lambda_{pr}W^2Q\{a\boldsymbol{i} + b\boldsymbol{j}\} \quad \ldots (\ 10\ )$$

Unsteady momentum force

$$(F_{un})_i = \lambda_{un}W\left\{-\frac{db}{d\xi}\boldsymbol{i} + \frac{da}{d\xi}\boldsymbol{j} + \frac{1}{\tan\gamma}\frac{dQ}{d\xi}\boldsymbol{k}\right\} \quad \ldots (\ 11\ )$$

Total aerodynamic force

$$F_{ae} = \chi\left[(F_{tu})_i + \left(F_{pr}\right)_i + (F_{un})_i\right] \quad \ldots (\ 12\ )$$

$$\bar{F}_{ae} = ml\Omega^2\, F_{ae} \quad \ldots (\ 13\ )$$

2.4 Rotordynamic Model

A 2D transfer matrix rotordynamic modelling approach developed by Myklestad [20], Prohl [21], Lund and Orcutt [22], is used together with the aerodynamic forces induced by fouling as an external forcing functions to determine the vibration response of the compressor rotor under different conditions of compressor fouling.

In the transfer matrix approach, the rotor bearing system is represented as a series of connected massless elastic shafts (field matrix) and concentrated point masses (point matrix) representing inertia elements (e.g. bladed disc, impellers, etc.), bearing forces, shaft discontinuities, gyroscopic effects, etc. This is depicted in Figure 6.

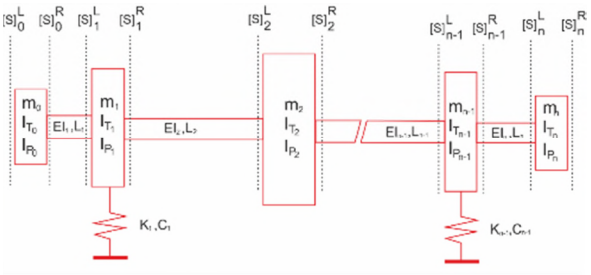

Figure 6 Basic transfer matrix rotor structure

Mathematically, the transfer matrix of a rotor-bearing system is represented as:

$$\{S\}_n = [U]\{S\}_0 \quad \ldots (\ 14\ )$$

where

$$\{S\}_i = [-y\ \varphi\ M_y\ V_y \vdots -x\ \theta\ M_x\ V_x \vdots 1] \quad \ldots (\ 15\ )$$

3.0 RESULTS AND DISCUSSIONS

3.1 Generalized Compressor Pressure-rise Characteristic

The generalized compressor pressure-rise characteristic represents the relationship between the pressure-rise coefficient and the non-dimensional flow coefficient.

The standard compressor pressure map in Figure 7 is transformed to the generalized form in Figure 8 based on the following conversion scheme:

$$\Psi = \frac{P_1(PR-1)}{\rho U^2} \quad \ldots (\ 16\ )$$

$$\Phi = \frac{\dot{m}}{\rho A_c U} \quad \ldots (\ 17\ )$$

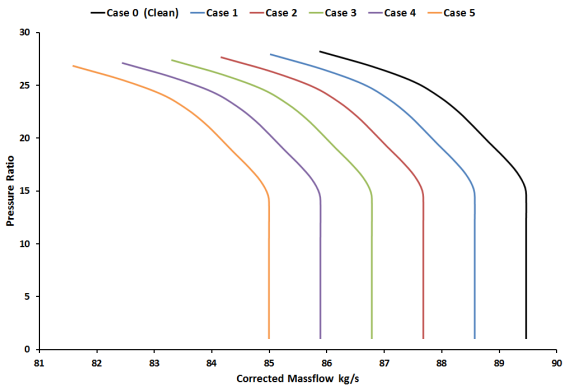

Figure 7 Clean & Fouled Comp. Press. Map for CN=1.02

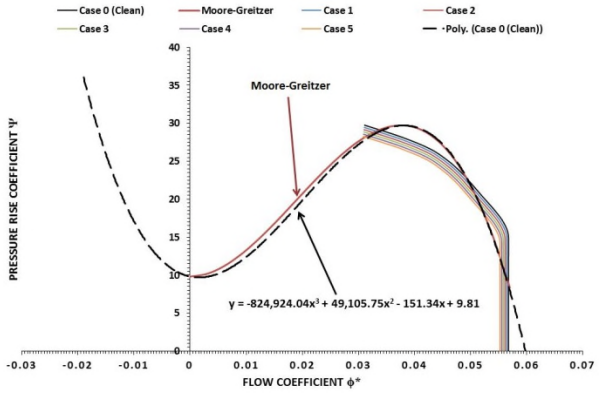

Figure 8 Generalized Comp. Press. Map

Based on Moore and Greitzer [13] recommendation for the general form of the expression for the generalized compressor pressure-rise characteristics, a polynomial curve is performed in the Figure 8 from which the relevant parameters for the Moore-Greitzer model compressor pressure-rise characteristic expression is summarized in Table 3.

Table 3
Moor-Greitzer compressor pressure-rise characteristic expression parameters

S/N	Parameters	Value
1	Semi-height of the cubic axisymmetric characteristic (H)	9.96
2	Semi-width of the cubic axisymmetric characteristic (W)	0.0188
3	Aspect ratio of the pressure-rise characteristic (S = H/W)	529.787
4	Shut-off value of the pressure-rise coefficient ψ_{co}	9.811

3.2 Compressor Disturbed Flow Coefficient Analysis

The required fouling parameters (FP) for the different cases of fouling considered and the simulated compressor inertia parameter $\{\lambda = (Nl)/(R\cos\gamma)\}$ is presented in Table 4 and Table 5 respectively for the solution of Equation (5).

Table 4
Fouling parameters for the various compressor fouling conditions considered

S/N	Cases	Fouling Parameter
1	Case 1	0.0299
2	Case 2	0.0597
3	Case 3	0.0896
4	Case 4	0.1194
5	Case 5	0.1493

Table 5
Simulated compressor inertia parameter

S/N	Parameter	Value
1	Inertia parameter (λ)	2.8243

The solutions of Equation (5) for the amplitudes of disturbed flow coefficient for the different cases of fouling are presented in Figure 9 - Figure 11.

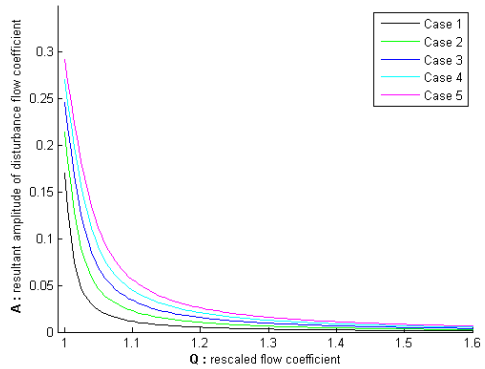

Figure 9 Resultant amplitude of disturbed flow coeff.

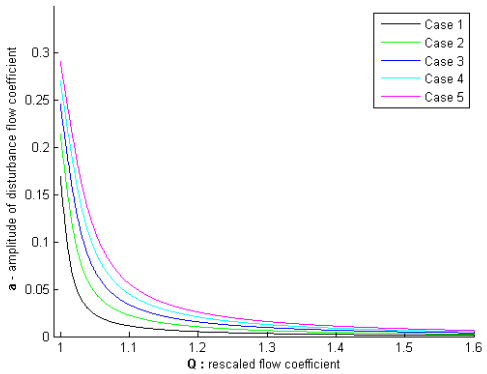

Figure 10 'a' amplitude of disturbed flow coeff.

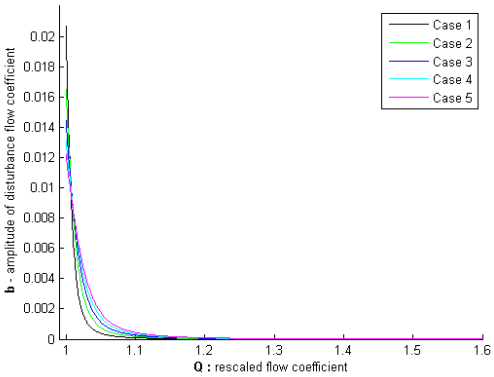

Figure 11 'b' amplitude of disturbed flow coeff.

3.3 Aerodynamic Force Analysis

For this work, a steady state condition in the compressor is assumed; as such, the unsteady momentum force is ignored in this analysis.

The relevant parameter for the solution of Equations (8) – (10) is summarized in Table 6.

Table 6
Relevant parameters for the aerodynamic force analysis [19]

λ_{tu}	92.6150	λ_{pr}	34.4968	τ_{c1}	-0.8254	τ_{c2}	1.9392	τ_{c3}	-0.8774

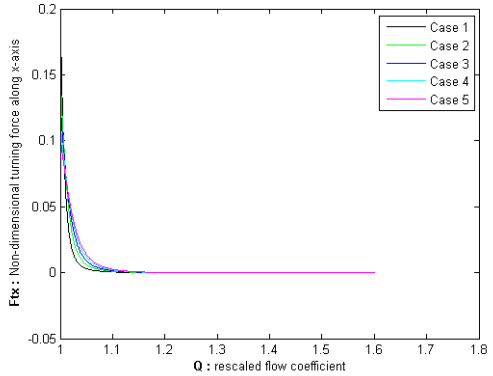

Figure 12 Non-Dimensional turning force along the x-Axis

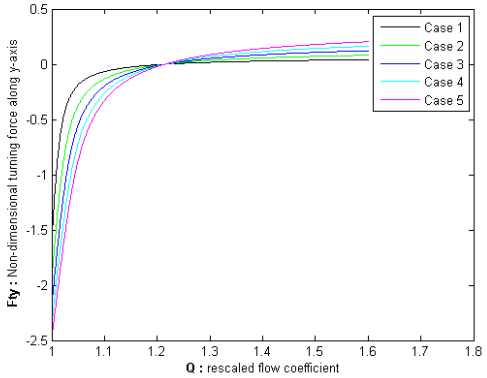

Figure 13 Non-Dimensional turning force along the y-Axis

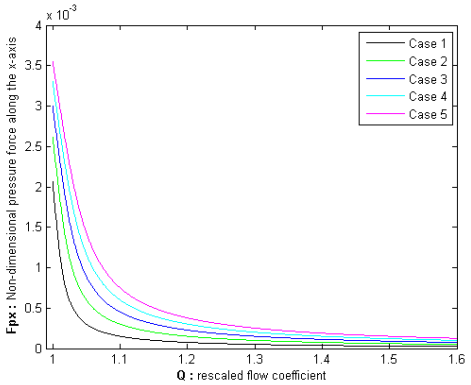

Figure 14 Non-Dimensional pressure force along the x-Axis

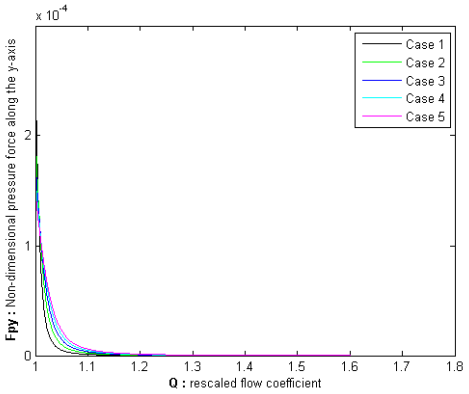

Figure 15 Non-Dimensional pressure force along the y-Axis

3.4 Rotordynamic Response Analysis

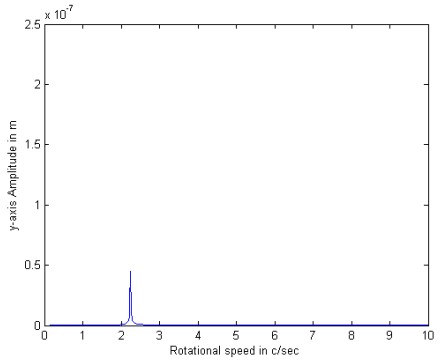

Figure 16 Case 1 engine vibration response @ Q = 1.2

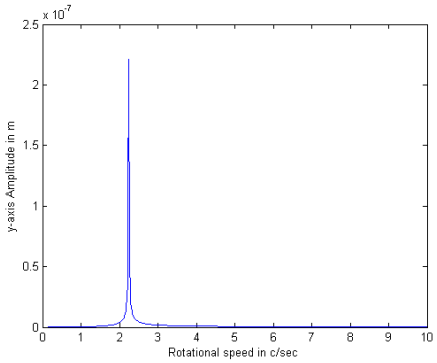

Figure 17 Case 5 engine vibration response @ Q = 1.2

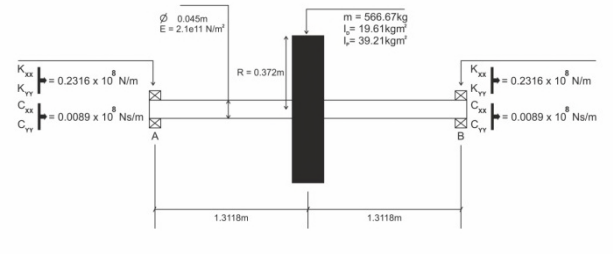

Figure 18 Simulated engine as a modified Jeffcott rotor

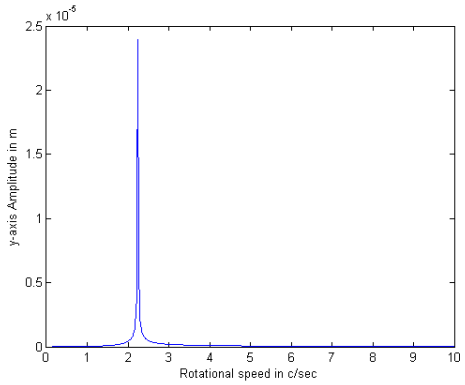

Figure 19 Case 5 engine vibration response @ Q = 1.0

Figure 9, Figure 10 and Figure 11shows the evolution of the amplitudes of the disturbed flow coefficient for different conditions of fouling in the simulated compressor engine.

Over the operating range from 1<Q <1.6, where Q=1.2 is the design point and Q=1 is the surge point, it is observed that for every case of fouling considered, the amplitude of the disturbed flow coefficient increases as the massflow is reduced or engine is throttled down. As the aerodynamic forces are function of the disturbed flow coefficient, there would be a marked increase in the vibration of the compressor.

From Figure 12, Figure 13, Figure 14 and Figure 15, it can be observed that the turning force is the major contributor to the aerodynamic force in the fouled compressor, with the pressure force having a negligible contribution. This observation also follows suit with the work by Alford [10] on the destabilizing aerodynamic forces in a turbine rotor due to clearance changes around its periphery.

Finally, the rotordynamic response analysis of the fouled compressor reveals some diagnostic information. It is observed from Figure 16 and Figure 17, at the operating design point of the compressor (i.e. Q = 1.2) for the various fouled operating conditions, the vibration response amplitude of the compressor at the compressors first fundamental frequency increases.

When the operating point is also varied to the surge point (i.e. Q=1.0), as shown in Figure 19, there is a further marked increase in the vibration amplitude at the compressor first fundamental frequency. As compared to the amplitude at the design operating point, this vibration would be more intense. This is as expected of a compressor operating in surge.

4.0 CONCLUSIONS

A methodology for studying the interaction between the aerodynamic and rotordynamic domain in a compressor due to fouling has been described. It is shown that the turning force is the main contributory component of the compressor aerodynamic force. It is concluded in this study that by monitoring the vibration response amplitude at the first fundamental frequency of the compressor rotor in combination with gas path analysis, fouling in the compressor can be effectively monitored.

5.0 REFERENCES

1. Zachary J. Advanced Gas Turbine Technology for Power Generation - Revolution or Evolution ? ISO Focus. June 2008; : 26–29.

2. Boyce MP., Latcovich JA. Condition Monitoring and Its Effect on the Life of New Advanced Gas Turbines. ASME-IGTI Glob. Gas Turbine News. 2002; 42(3): 4–10.

3. Meher-homji CB., Cullen JP. Integration of Condition Monitoring Technologies for the Health Monitoring of Gas Turbines. ASME 1992 International Gas Turbine and Aeroengine Congress and Exposition. Cologne, Germany: ASME; 1992. p. V005T15A007. Available at: DOI:10.1115/92-GT-052

4. Li YG. Performance Analysis Based Gas Turbine Diagnostics: A Review. Journal of Power and Energy. 2002; 216(5): 363–377.

5. Meher-homji CB., Focke AB. Performance & Vibration Monitoring for the Prevention of Gas Turbine Airfoil Failures. 6th Bi annual ASME Conference on Failure Prevention & Reliability, September, 1985 ASME Vol H-331. 1985.

6. Biliotti D., Bianchini A., Vannini G., Belardini E., Giachi M., Tapinassi L., et al. Analysis of the Rotordynamic Response of a Centrifugal Compressor Subject to Aerodynamic Loads Due to Rotating Stall. Journal of Turbomachinery. 2015; 137(2): 21002. Available at: DOI:10.1115/1.4028246

7. Meher-Homji CB., Bromley A. Gas Turbine Axial Compressor Fouling and Washing. Proceedings of the Thirty-Third Turbomachinery Symposium. 2004. pp. 163–191.

8. Igie U., Pilidis P., Fouflias D., Ramsden K., Laskaridis P. Industrial Gas Turbine Performance: Compressor Fouling and On-Line Washing. Journal of Turbomachinery. 2014; 136(10): 101001–101013. Available at: DOI:10.1115/1.4027747

9. Meher-homji CB., Focke AB., Wooldridge MB. Fouling of Axial Flow Compressors - Causes, Effcets, Detention, And Control. Proceedings of the Eighteenth Turbomachinery Symposium. Texas A&M University, Texas, USA; 1989. pp. 55–76.

10. Alford JS. Protecting Turbomachinery From Self-Excited Rotor Whirl. Journal of Engineering for Power. 1965; 87(4): 333–343.

11. Weigl H. Active Stabilization of Rotating Stall and Surge in a Transonic Single Stage Axial Compressor, PhD. Thesis. Massachusetts Institute of Technology; 1997.

12. Tryfonidis M., Etchevers O., Paduano JD., Epstein AH., Hendricks GJ. Prestall Behavior of Several High-Speed Compressors. Journal of Turbomachinery. 1995; 117(1): 1–24.

13. Greitzer EM., Moore FK. A Theory of Post-Stall Transients in Axial Compression Systems : Part I — Development of Equations. Transactions of the ASME. 1986; 108(68).

14. Al-Nahwi AA. Aerodynamic-Rotordynamic Interaction in Axial Compression System. PhD Thesis. Massachusetts Institute of Technology; 2000.

15. Yoon SY., Lin Z., Allaire PE. Control of Surge in Centrifugal Compressors by Active Magnetic Bearings. Advances in Industrial Control. London: Springer-Verlag; 2013. pp. 1–275. Available at: DOI:10.1007/978-1-4471-4240-9

16. Gravdahl JT., Egeland O. A Moore-Greitzer axial compressor model with spool dynamics. Proceedings of the 36th Conference on Decision & Control, San Diego, California, USA. December, 1997. IEEE; 1997.

17. Fink DA., Cumpsty NA., Greitzer EM. Surge Dynamics in a Free Spool Centrifugal Compressor System. Journal of Turbomachinery. 1992; 114: 321–332.

18. Gravdahl JT., Egeland O. Control of the Three-State Moore-Greitzer Compressor Model Using a Close-Coupled Valve. Proceedings of the 1997 European Control Conference, July 1997. 1997.

19. Jombo G. Towards Gas Turbine Prognosis with Vibration and Gas Path Analysis. PhD Thesis. Cranfield University; 2017.

20. Myklestad NO. A New Method of Calculating Natural Modes of uncoupled Bending Vibrations of Airplane Wings and Other Types of Beams. Journal of the Aeronautical Sciences. 1944; 11(2): 153–162.

21. Prohl MA. A General Method for Calculating Critical Speeds of Flexible Rotors. Journal of Applied Mechanics. 1945; 67: A-142-A-148.

22. Lund JW., Orcutt FK. Calculations and Experiments on the Unbalance Response of a Flexible Rotor. Journal of Engineering for Industry. 1967; 89(4): 785–796.